Environmental Science & Technology

Article

Cite This: Environ. Sci. Technol. 2019, 53, 8883−8891

pubs.acs.org/est

Mineral Defects Enhance Bioavailability of Goethite toward Microbial Fe(III) Reduction

Luiza Notini,[†] James M. Byrne,[‡] Elizabeth J. Tomaszewski,[‡] Drew E. Latta,[†] Zhe Zhou,[†] Michelle M. Scherer,[†] and Andreas Kappler*[,‡]

[†]Department of Civil and Environmental Engineering, University of Iowa, Iowa City, Iowa 52242, United States

[‡]Geomicrobiology Group, Centre for Applied Geosciences (ZAG), University of Tübingen, Sigwartstrasse 10, D-72076, Tübingen, Germany

Supporting Information

ABSTRACT: Surface defects have been shown to facilitate electron transfer between Fe(II) and goethite (α-FeOOH) in abiotic systems. It is unclear, however, whether defects also facilitate microbial goethite reduction in anoxic environments where electron transfer between cells and Fe(III) minerals is the limiting factor. Here, we used stable Fe isotopes to differentiate microbial reduction of goethite synthesized by hydrolysis from reduction of goethite that was further hydrothermally treated to remove surface defects. The goethites were reduced by *Geobacter sulfurreducens* in the presence of an external electron shuttle, and we used ICP-MS to distinguish Fe(II) produced from the reduction of the two types of goethite. When reduced separately, goethite with more defects has an initial rate of Fe(III) reduction about 2-fold higher than goethite containing fewer defects. However, when reduced together, the initial rate of reduction is 6-fold higher for goethite with more defects. Our results suggest that there is a suppression of the reduction of goethite with fewer defects in favor of the reduction of minerals with more defects. In the environment, minerals are likely to contain defects and our data demonstrates that even small changes at the surface of iron minerals may change their bioavailability and determine which minerals will be reduced.

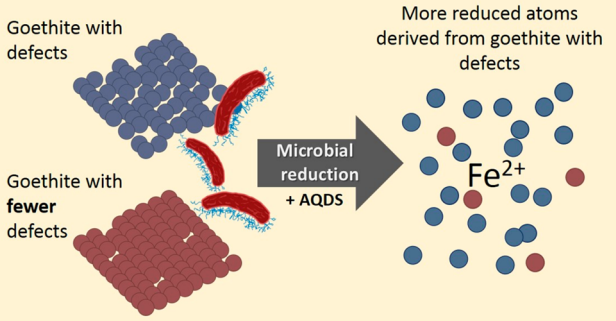

INTRODUCTION

In subsurface environments where oxygen is limiting, Fe(III)-reducing microorganisms can use Fe(III) mineral phases as terminal electron acceptors, forming reduced iron (Fe) species such as aqueous Fe(II) and Fe(II)-bearing minerals.[1−5] Microbial respiration of Fe(III) minerals is particularly important in Fe redox chemistry because it continuously regenerates Fe(II) that can further undergo electron transfer with Fe(III) (oxyhydr)oxides, controlling the cycling and availability of elements such as of C, N, and P.[5−12] Initial studies on microbial Fe(III) reduction showed that microorganisms could metabolize poorly crystalline Fe(III) (oxyhydr)oxides such as ferrihydrite.[13] Later on, it was demonstrated that Fe(III)-reducing microorganisms could also reduce more crystalline Fe(III) minerals such as goethite, hematite, magnetite, maghemite, lepidocrocite, and akaganéite.[3,14−20]

Crystalline Fe(III) (oxyhydr)oxides have low solubility at circumneutral pH values, which limits the bioavailability and therefore the extent of microbial Fe(III) reduction. Fe(III)-metabolizing bacteria, however, have evolved strategies to access the poorly soluble electron acceptors, such as direct cell-mineral contact, conductive pili (nanowires), release of chelating compounds to solubilize iron, or via extracellular electron shuttles that facilitate the transfer of electrons to the solid.[21−24] Electron shuttles such as natural organic matter and humic substances are present in natural environments and can accelerate Fe(III) (oxyhydr)oxide reduction.[25] However, the electron transfer from electron shuttle substances to Fe(III) minerals represents the rate-limiting step in microbial Fe(III) mineral reduction via electron shuttles.[26] Therefore, mineralogical properties such as crystallinity have an important role in the rate and extent of microbial Fe(III) reduction. For example, the rate of microbial Fe(III) reduction is linked to crystallinity, in that, short-range ordered phases, such as ferrihydrite, are reduced at faster rates than more crystalline minerals, such as goethite and hematite.[14,15,17,27−29] When comparing the microbial Fe(III) reduction of the same mineral but with different crystallinities, less crystalline phases have higher Fe(III) initial reduction rates.[15]

Mineral crystallinity may be altered in nature by the formation of surface defects. Surface defects arise from a deviation in the ideal composition and/or structure of a

Received: May 29, 2019
Revised: July 7, 2019
Accepted: July 9, 2019
Published: July 9, 2019

DOI: 10.1021/acs.est.9b03208
Environ. Sci. Technol. 2019, 53, 8883−8891

mineral.[30] Using surface-sensitive techniques (e.g., X-ray magnetic circular dichroism: XMCD and oxygen X-ray absorption: XAS), we have demonstrated that goethite synthesized by low-temperature Fe(III) hydrolysis is non-stoichiometric and contains defects from Fe vacancies.[31] In abiotic studies, surface defects have been shown to play an important role in mineral geochemistry.[31−34] Nonstoichiometric goethite undergoes facile Fe(II)−Fe(III) oxide electron transfer, depositing an additional layer of goethite.[31]

Faster reduction of less crystalline minerals[14,15,17,27−29] as well as the effect of defects on the mineral reactivity in abiotic systems[31] raise the question of whether surface defects will also influence microbial respiration of goethite. Here, we used a hydrothermal treatment to anneal goethite surface defects, as in our previous work.[31] In the present work, however, we used isotope-labeled minerals to investigate the role of defects on microbial Fe(III) reduction of goethite. Specifically, we tested whether the presence of defects leads to preferential use of this Fe(III) mineral as the electron acceptor for Fe(III) microbial reduction assisted by an extracellular electron shuttle.

METHODS

Goethite Synthesis. Natural Fe abundance goethite (referred to as ^{NA}goethite, contains 2.31 ± 0.001% of ^{57}Fe) and ^{56}Fe goethite (referred to as ^{56}goethite, contains virtually no ^{57}Fe) were prepared from natural abundance iron metal or ^{56}Fe-enriched Fe metal (Isoflex, 99.94% purity), respectively, following a modified version of Schwertmann and Cornell (see details SI).[35] Goethite was washed, centrifuged, freeze-dried, ground with a mortar and pestle, and passed through a 100 mesh sieve. The final mineral, as synthesized, will be referred to goethite$^{(AS)}$ and it is similar to the microgoethite used in our previous work.[36−41] The Brunauer−Emmett−Teller (BET) specific surface area of goethite$^{(AS)}$ (synthesized from natural abundant Fe) was determined by N_2 sorption at 77 K and found to be 28 $m^2\ g^{-1}$ for the ^{NA}goethite. XRD patterns showed that the material contains only goethite (Figure S8).

Hydrothermal Treatment. Goethite was subjected to a hydrothermal treatment to anneal defects.[31] A suspension of the goethite in deionized water was placed into a digestion bomb and kept in an oven at 150 °C for 44 h. The digestion bomb was allowed to cool to room temperature; the solids were centrifuged and freeze-dried and referred to as hydrothermally treated goethite (goethite$^{(HT)}$). Note that hydrothermally treated goethite is not sieved after the treatment, which causes it to have a slightly different state of aggregation. The BET specific surface area of goethite$^{(HT)}$ (synthesized from natural abundant Fe) was found to be 22 $m^2\ g^{-1}$. XRD patterns showed that the material contains only goethite, confirming that the hydrothermal treatment did not induce transformation of the goethite (Figure S8).

Microbial Fe(III) Reduction Experiments. *Geobacter sulfurreducens* was obtained from the laboratory stocks at the University of Tuebingen. For the respective experiments, *Geobacter sulfurreducens* cells were grown in 4 × 500 mL serum bottles at 30 °C (25 mM acetate, 40 mM fumarate) in bicarbonate-buffered (30 mM) anoxic medium containing KH_2PO_4 (4.4 mM), NH_4Cl (5.61 mM), $MgSO_4{\cdot}7H_2O$ (2 mM), and $CaCl_2{\cdot}2H_2O$ (0.68 mM). The medium was amended with 1 mL L^{-1} trace-element solution SL 10, 1 mL L^{-1} selenite-tungstate solution, and 0.5 mL L^{-1} of 7-vitamin solution and was flushed with a N_2/CO_2 (80/20, v/v) gas mixture; the pH of the final anoxic medium was ∼7. Late log phase (1 week) cultures were harvested by centrifugation at 5000 rpm (20 min, 10 °C), washed twice using 30 mM bicarbonate buffer, and concentrated into a pellet.

For the experiments, 50 mL serum bottles with 25 mL of anoxic medium and 50 mg (2 g L^{-1}) of goethite (or hydrothermally treated goethite or a mix) were prepared. Sodium acetate (4 mM) was used as an electron donor, and 9,10-anthraquinone-2,6-disulfonic acid disodium salt (AQDS; 10 μM) was added to the microcosms to act as an extracellular electron shuttle. Aliquots of the washed cells were used to inoculate the reactors with ∼10^8 cells mL^{-1}. The number of cells was estimated based on a correlation between optical density and flow cytometry measurements. Bottles were incubated (stationary) at 20 °C in the dark for 20−41 days, and 0.6 mL of the slurry was periodically sampled, with the aqueous and solids phases separated by centrifugation (12000 rpm, 15 min). The reacted solids were subjected to a sequential extraction procedure using 1 M sodium acetate (pH 5, 24 h) followed by 0.5 M HCl (2 h). The aqueous and extracted samples were subjected to subsequent Fe(II) and total Fe analysis using the 1,10-phenanthroline method.[42]

Samples were taken at 5 and 28 days of incubation and characterized by scanning electron microscopy (SEM, Jeol JSM-6500F) operated at 5 kV, 10 mm working distance. Samples were fixed in glutaraldehyde (2.5%) at 4 °C overnight, followed by dehydration in an increasing ethanol series (30, 50, 70, 95, and 100% twice), and they were finally washed in hexamethyldisilazane (HMDS).[43] Samples were also taken after 20 days for analysis by XRD and Mössbauer spectroscopy (see SI for details).

Additional microbial Fe(III) reduction experiments were prepared in triplicates using 1 and 0.5 g L^{-1} goethite instead of the original 2 g L^{-1}. For those reactors, the ratio of acetate/Fe was maintained.

Isotope-Labeled Microbial Fe(III) Reduction. Isotope-labeled ^{56}Fe and ^{NA}Fe were used to differentiate goethite$^{(AS)}$ and goethite$^{(HT)}$. Specifically, three reactors contained a mix of 25 mg of ^{56}goethite$^{(AS)}$ and 25 mg of ^{NA}goethite$^{(HT)}$, whereas the other three reactors contained 25 mg of ^{NA}goethite$^{(AS)}$ with defects and 25 mg of ^{56}goethite$^{(HT)}$. Other than the isotope composition of goethite, the experiments were performed as described for microbial Fe(III) reduction experiments. The aqueous phase (supernatant after centrifuging reactor) and the sodium acetate extract (supernatant after centrifuging sodium acetate extraction) were combined, and the Fe isotope composition analysis was performed with a quadrupole inductively coupled plasma-mass spectrometer (ICP-MS, Agilent 7900) using He gas in collision cell mode to remove isobaric interferences (predominantly $^{40}Ar^{16}O$ and $^{40}Ar^{16}O^{1}H$) for ^{56}Fe and ^{57}Fe.

Isotope-Labeled Chemical Reduction. Six reactors containing a mix of 25 mg of ^{56}goethite$^{(AS)}$ and 25 mg of ^{NA}goethite$^{(HT)}$ were prepared. Half of the samples were mixed with DI water and freeze-dried, while the other half was used with no extra steps. Both freeze-dried solids and the regular solids were submitted to the same chemical reduction experiment using partial additions (0.3 mL) of a solution of 20 mM $Na_2S_2O_4$ to reduce goethite. Between each $Na_2S_2O_4$ addition, a sample of the aqueous phase was collected and analyzed by phenanthroline and ICP-MS.

DOI: 10.1021/acs.est.9b03208
Environ. Sci. Technol. 2019, 53, 8883−8891

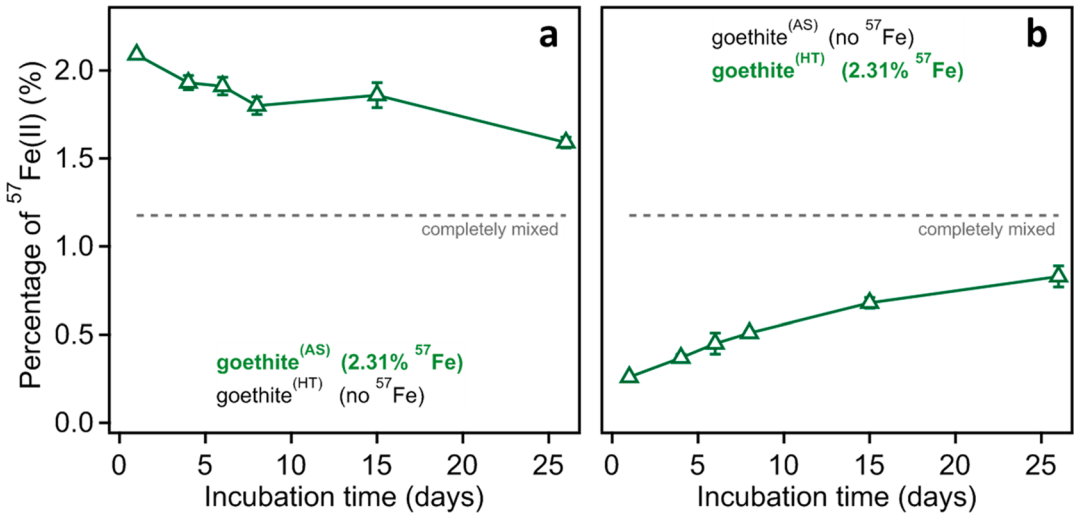

Figure 1. Percentage of ^{57}Fe isotope in reduced iron (Fe(II)) from reactors containing a labeled mix of goethite$^{(AS)}$ and goethite$^{(HT)}$. In panel a, goethite$^{(AS)}$ is labeled with the ^{57}Fe isotope, while in panel b, goethite$^{(HT)}$ is labeled with the ^{57}Fe isotope. Data corresponds to an average of biological triplicates, and the error bars indicate standard deviations. Experimental conditions: 10^8 cells mL^{-1} *Geobacter sulfurreducens*; 10 μM AQDS; (a) 1 g L^{-1} ^{NA}goethite$^{(AS)}$ + 1 g L^{-1} ^{56}goethite$^{(HT)}$ or (b) 1 g L^{-1} ^{56}goethite$^{(AS)}$ + 1 g L^{-1} or ^{NA}goethite$^{(HT)}$.

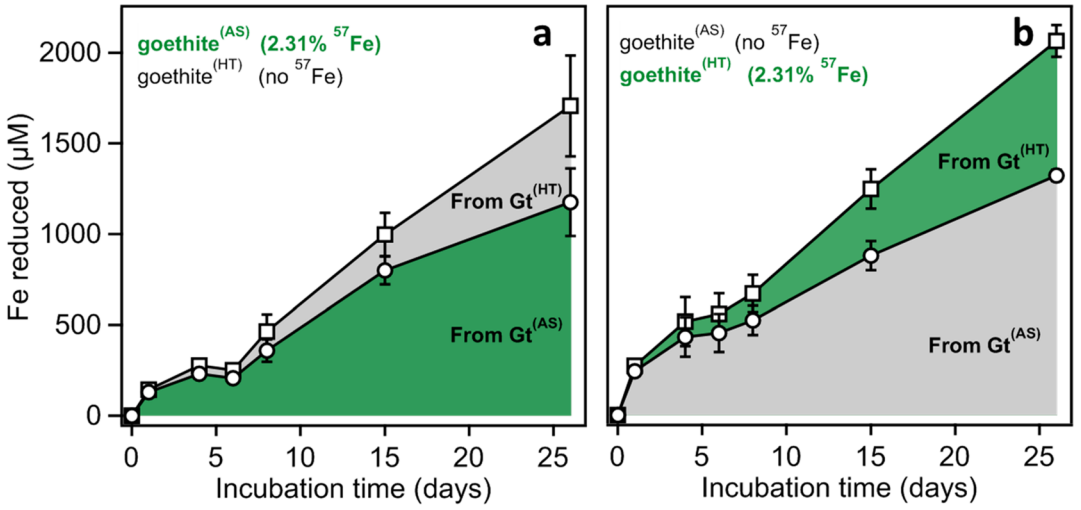

Figure 2. Origin of the reduced iron (Fe(II)) based on isotope signature and concentration of the microbially reduced Fe from reactors containing a labeled mix of goethite$^{(AS)}$ and goethite$^{(HT)}$. Data corresponds to an average of biological triplicates, and the error bars indicate standard deviations. Experimental conditions: 10^8 cells mL^{-1} *Geobacter sulfurreducens*; 10 μM AQDS; (a) 1 g L^{-1} ^{NA}goethite$^{(AS)}$ + 1 g L^{-1} ^{56}goethite$^{(HT)}$ or (b) 1 g L^{-1} ^{56}goethite$^{(AS)}$ + 1 g L^{-1} ^{NA}goethite$^{(HT)}$.

RESULTS AND DISCUSSION

Microbial Fe(III) Reduction of Isotope Labeled Goethite with and without Defects (Together). To evaluate whether goethite (α-FeOOH) with more defects is preferentially reduced by *Geobacter sulfurreducens* in the presence of AQDS, we synthesized goethite containing defects and goethite with fewer defects. Goethite was synthesized by hydrolysis (goethite$^{(AS)}$), which has been shown to form mineral containing surface defects.[31] We further hydrothermally treated the goethite to obtain a mineral with fewer defects (goethite$^{(HT)}$).[31] We inoculated a mixture of goethite$^{(AS)}$ and goethite$^{(HT)}$ with *Geobacter sulfurreducens* in the presence of AQDS. Specifically, we used equal amounts of goethite$^{(AS)}$ synthesized with naturally abundant iron (2.31 ± 0.001% of ^{57}Fe) and goethite$^{(HT)}$ synthesized from ^{56}Fe-enriched Fe metal (virtually no ^{57}Fe). The isotopic composition of the goethite mixture before inoculation had an average concentration of 1.18 ± 0.07% ^{57}Fe (dashed line in Figure 1). Having a mixture of goethite minerals with different isotopic compositions allowed us to track the origin of the reduced Fe during microbial respiration.

We measured the isotopic composition of the aqueous and sodium acetate extracted Fe produced from microbial reduction of Fe(III) over time (Figure 1a). Virtually no Fe(III) was found in aqueous and extracted samples (<7%), and most of the Fe(II) was recovered in the acetate extraction rather than in the aqueous phase. The isotope composition showed that initially 2.09 ± 0.01% of the iron present in the aqueous and extracted Fe(II) fraction was ^{57}Fe. Over 26 days, the ^{57}Fe concentration in the Fe(II) fraction decreased but never reached the completely mixed isotopic composition of the goethite mixture (1.18%). ^{57}Fe concentrations greater than the completely mixed value of 1.18% indicate that more goethite$^{(AS)}$ was reduced than goethite$^{(HT)}$. If equal amounts of

DOI: 10.1021/acs.est.9b03208
Environ. Sci. Technol. 2019, 53, 8883−8891

goethite$^{(AS)}$ and goethite$^{(HT)}$ were reduced, the isotope signature of Fe reduced would be constant at ^{57}Fe = 1.18%. Note that the data in each point in time reflects the isotopic composition of the cumulative Fe(II) reduced throughout the experiment and not the isotopic composition of the Fe being reduced at that time point specifically.

While the isotopic data appear to indicate more reduction of goethite$^{(AS)}$ (i.e., goethite with more defects) it is possible that isotopic fractionation may have contributed to the enhanced reduction of lighter isotopes, as observed in many biological and chemical processes.[44,45] For example, dissimilatory Fe(III) (oxyhydr)oxide reduction has been shown to cause isotope fractionation.[46,47] More specifically, the aqueous Fe(II) reduced through microbial activity has been shown to have a lower ^{56}Fe/^{54}Fe ratio than the initial Fe(III) (oxyhydr)oxide substrate. It has been suggested that fractionation might derive from a preference to sorb heavier isotopes that can further undergo electron transfer forming a new layer of mineral.[47] Moreover, reaction of newly reduced Fe atoms and the Fe(III) oxides can lead to isotopic mixing.[40]

To test whether enhanced reduction of goethite with defects was due to differences between goethite$^{(AS)}$ and goethite$^{(HT)}$ or an effect of preferential use of isotopes, we reversed the isotope labeling of the different goethite minerals and measured the isotopic composition of the reduced Fe formed from microbial respiration (Figure 1b). Here, we did not explore the mechanisms of isotopic fractionation but rather focused on the possibility that preferential reduction of one isotope could have made our data biased. This time, we synthesized goethite$^{(HT)}$ from naturally abundant Fe (2.31% of ^{57}Fe) and goethite$^{(AS)}$ from ^{56}Fe, therefore all ^{57}Fe present in the reactor was in goethite$^{(HT)}$. The isotopic composition of the Fe(II) formed upon microbial reduction of the goethite mixture began at 0.26 ± 0.00% and increased over time but never reached the 1.18% ^{57}Fe, indicating that more goethite$^{(AS)}$ was reduced than goethite$^{(HT)}$.

To compare the switched isotope experiments, we calculated what percent of the reduced Fe originated from each goethite based on the ^{57}Fe concentration of the reduced Fe (see discussion in SI). Then the percentage of atoms originating from goethite$^{(AS)}$ and goethite$^{(HT)}$ were multiplied by the total μM of reduced Fe (Figure 2). This allows us to compare the results from the switched isotope experiments independent of which goethite was labeled with ^{57}Fe (green shaded area), and the results are remarkably similar. Our approach further confirmed that different isotopes did not cause goethite to have more or fewer defects. Note that on the first experiment, goethite$^{(HT)}$ was made from the lighter isotopes, therefore, it could be favored by isotopic fractionation. In the second experiment, goethite$^{(AS)}$ was made from the lighter isotopes. However, for both isotope experiments, the area that represents atoms derived from goethite$^{(AS)}$ is substantially larger than the area that represents atoms derived from goethite$^{(HT)}$. Switching the goethite isotope labels appears to have no effect on the origin of Fe(II) formed from microbial respiration of the goethite mixture. This provides compelling evidence that the preferential reduction of goethite$^{(AS)}$ is not a result of isotopic fractionation but is instead related to the mineral's properties.

Two additional factors that might contribute to the preferential reduction of goethite$^{(AS)}$ include surface area and aggregation. Past studies suggested that Fe(III) mineral reactivity toward microbial species is strongly influenced by reactive surface area.[2,48] The goethites used here, however, have similar surface areas (BET surface are for goethite$^{(AS)}$ = 28 m^2 g^{-1} and goethite$^{(HT)}$ = 22 m^2 g^{-1}). If the preferential reduction of goethite with defects were only a function of surface area, we should expect 56% (28/(28 + 22)) of the Fe(II) from goethite$^{(AS)}$ and 44% (22/(28 + 22)) from goethite$^{(HT)}$. Instead, we observed initially 90% of the reduced atoms arise from goethite with more defects. The preparation of goethite$^{(AS)}$ included a sieving step; however, goethite$^{(HT)}$ was not ground and sieved because this step has been shown to reintroduce defects to goethite.[31] As a consequence, goethite$^{(HT)}$ was in chunks while goethite$^{(AS)}$ was not. To test if sieving goethite$^{(AS)}$ but not sieving goethite$^{(HT)}$ influenced our experiment, we freeze-dried both goethites together, which resulted in both goethites forming chunks. For the goethites that were not freeze-dried, only the ^{NA}goethite$^{(HT)}$ was in chunks. Both freeze-dried solids and not freeze-dried goethites were reduced with $Na_2S_2O_4$, and the isotope signature of reduced Fe atoms was similar, independent of whether the aggregations were similar or different (Figure S1). These results demonstrate that the sieving/not sieving does not explain the preferential reduction of goethite. Together our findings suggest that, when using an electron shuttle, the presence of surface defects enhances the bioavailability of goethite toward microbial Fe(III) reduction.

Microbial Fe(III) Reduction of Goethite with and without Defects (Separately). To explore whether the enhanced reduction of goethite with defects was simply due to faster reduction of goethite$^{(AS)}$ than goethite$^{(HT)}$, we measured the rates of microbial Fe(III) reduction of each goethite separately. We prepared incubations which varied the type of goethite (goethite$^{(AS)}$ and goethite$^{(HT)}$) and the presence of the extracellular electron shuttle, AQDS. In the presence of AQDS, goethite$^{(AS)}$ was reduced at a faster initial rate (2.0×10^{-7} mol L^{-1} min^{-1} m^{-2}) than goethite$^{(HT)}$ (0.8×10^{-7} mol L^{-1} min^{-1} m^{-2}) (Figures 3 and S2). However, after 41 days, the extent of Fe(III) reduction was similar for both types of goethite (goethite$^{(AS)}$ = 13.44 ± 0.77%; goethite$^{(HT)}$ = 10.71 ± 1.10%). The extent of goethite reduction is the same if normalized by surface area, indicating that the presence of defects leads to faster initial reduction but not more reduction at the end of the experiment.

In the absence of AQDS, Fe(III) initial reduction rate was 4.2×10^{-8} mol L^{-1} min^{-1} m^{-2} for goethite$^{(AS)}$ and 3.3×10^{-8} mol L^{-1} min^{-1} m^{-2} for goethite$^{(HT)}$. The extent of Fe(III) reduction stabilized after 10 days, at 1.64 ± 0.33% for goethite$^{(AS)}$ and 0.62 ± 0.06% for goethite$^{(HT)}$. When AQDS was added as an electron shuttle, microbial reduction of both goethites have faster initial rates and larger extents of Fe(III) reduction than in the absence of AQDS.[15] Interestingly though, both in the presence or in the absence of AQDS, surface defects influenced initial rates of Fe(III) reduction. These results suggest the presence of defects facilitates the microbial Fe(III) reduction of goethite independent of whether the electron is injected into the Fe(III) mineral directly via enzymatic activity (by a cell that is attached to the mineral) or abiotically via the reduced form of the electron shuttle, i.e., AH_2QDS. The faster initial rates of microbial Fe(III) reduction for goethite$^{(AS)}$ when compared to goethite$^{(HT)}$ (Figure 3) is consistent with previous works that showed initial rates of Fe(III) microbial reduction are inversely proportional to the crystallinity of minerals.[16,17]

DOI: 10.1021/acs.est.9b03208
Environ. Sci. Technol. 2019, 53, 8883−8891

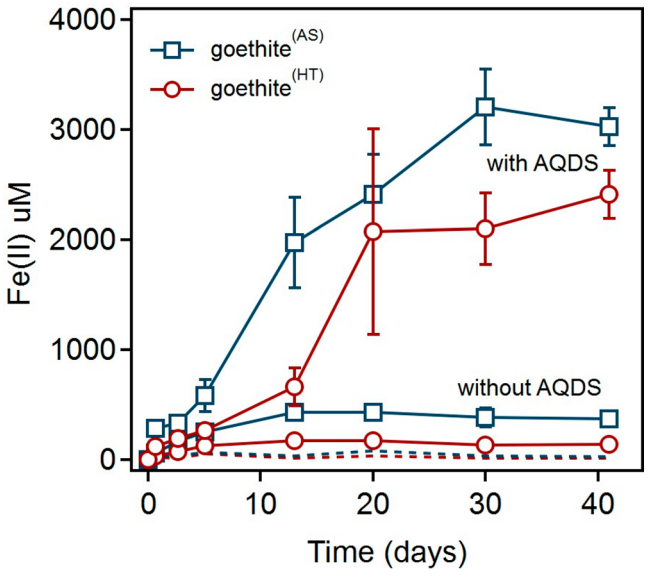

Figure 3. Microbial Fe(III) reduction of either goethite$^{(AS)}$ or goethite$^{(HT)}$, in separate setups, in the presence and in the absence of AQDS. Dashed line represents abiotic control for goethite$^{(AS)}$ (blue) and goethite$^{(HT)}$ (red). Data corresponds to average of biological triplicates, and the error bars indicate standard deviations. Experimental conditions: 2 g L^{-1} goethite$^{(AS)}$ or goethite$^{(HT)}$; 0 (abiotic controls) or 10^8 cells mL^{-1} *Geobacter sulfurreducens*; 0 or 10 μM AQDS.

Total Fe(II) in noninoculated reactors (abiotic controls) was below 0.3% of the total iron throughout the experiment (Figure 3, dashed line). Note that, for inoculated reactors, Fe(II) quantification may be underestimated as Fe(II) sorbed to the inside glass walls of the bottles. This was confirmed by adding phenanthroline to an emptied glass bottle which immediately revealed the presence of Fe(II) (Figure S3). The same procedure was repeated for an abiotic control and showed no presence of Fe(II).

To evaluate if Fe(III) reduction was related to goethite concentration, we inoculated the reactors with varying concentrations of goethite$^{(AS)}$ or goethite$^{(HT)}$) (Figure S4) and calculated the instantaneous rates of reduction using different goethite concentrations (Figure S5). Independent of the goethite concentration, the rate of Fe(III) reduction decreases to almost zero, followed by a sharp increase, which can be observed in Figure S5 and in the plateau in Figures 3 and S4. To evaluate if changes in the rate of Fe(III) reduction are related to the removal of the first layer of Fe atoms, we compared the reduction of Fe(III) with the number of atoms at the surface. Assuming that goethite surfaces are dominated by exposure of (101) and (001) crystallographic faces,[49] goethite$^{(AS)}$ has 5.04−5.54% of the Fe atoms at the surface, while goethite$^{(HT)}$ has 3.96−4.35% (see details in SI) and the shaded area in Figure S4 represents the percentage of atoms at the surface. It is remarkable that independent of the presence of defects, the change in the rate of Fe(III) reduction happened when 2−4% of the total iron was removed and therefore before all Fe atoms from the first layer could have possibly been removed. Perhaps, reduction of goethite is localized, and the removal of the first layer of atoms at this region is enough to increase the rate of microbial Fe(III) reduction.

Isotope Data Demonstrates More Reduction of Goethite with Defects than Predicted. To probe whether the linear combination of reduction of goethite$^{(AS)}$ and goethite$^{(HT)}$ can explain enhanced reduction of goethite with defects observed in our isotope-labeled experiment, we built a model that consists of adding the average concentration of Fe(II) formed for reduction of 1 g L^{-1} of both goethites *separately* (values from Figure S4). We then compared those with isotope experiments (average of switched isotope experiments), where 1 g L^{-1} of goethite$^{(AS)}$ and goethite$^{(HT)}$ were added *together* in the bottle. The total Fe(II) reduced in this experiments was remarkably similar, independent of whether the reduction happened in two separate bottles or in the same bottle using isotopes (Figure 4a). However, when we compare the fraction of Fe(II) that derived from goethite$^{(AS)}$ (area above line) or goethite$^{(HT)}$ (area below line), there was a clear difference (Figure 4b). For the experiment where reduction happened separately (hatched area), reduction of goethite$^{(AS)}$ had a similar pattern but slightly higher values than the reduction of goethite$^{(HT)}$ (area below dashed line). However, when reduction happens

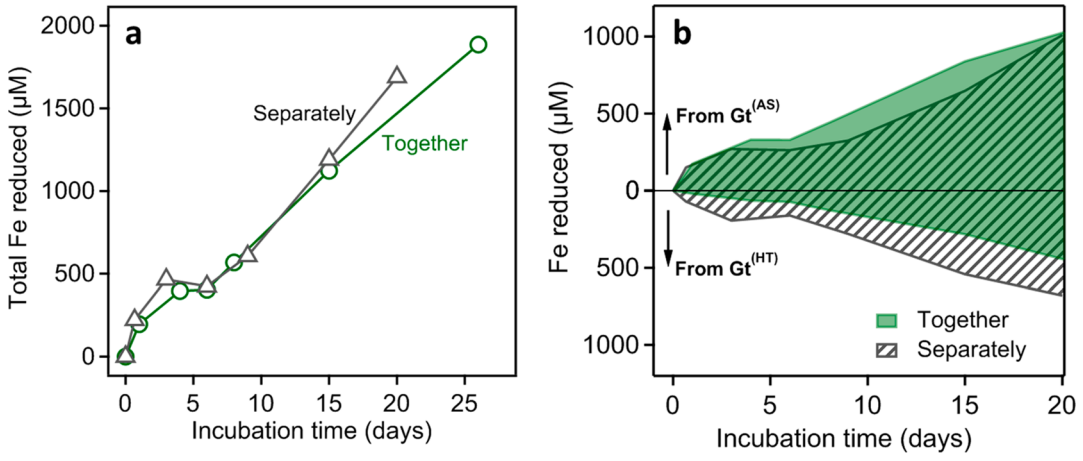

Figure 4. (a) Total Fe(II) reduced by microbial Fe(III) reduction of goethite$^{(AS)}$ and goethite$^{(HT)}$ when inoculated separately or together and (b) diagram revealing the origin of the reduced atoms for the reduction of goethite$^{(AS)}$ and goethite$^{(HT)}$ when inoculated separately or together. Experimental conditions: 10^8 cells mL^{-1} *Geobacter sulfurreducens*; 10 μM AQDS; 1 g L^{-1} goethite$^{(AS)}$ + 1 g L^{-1} goethite$^{(HT)}$ in separate bottles (separately); 2 g L^{-1} of isotope labeled mix of goethite$^{(AS)}$ and goethite$^{(HT)}$ (together).

DOI: 10.1021/acs.est.9b03208
Environ. Sci. Technol. 2019, 53, 8883−8891

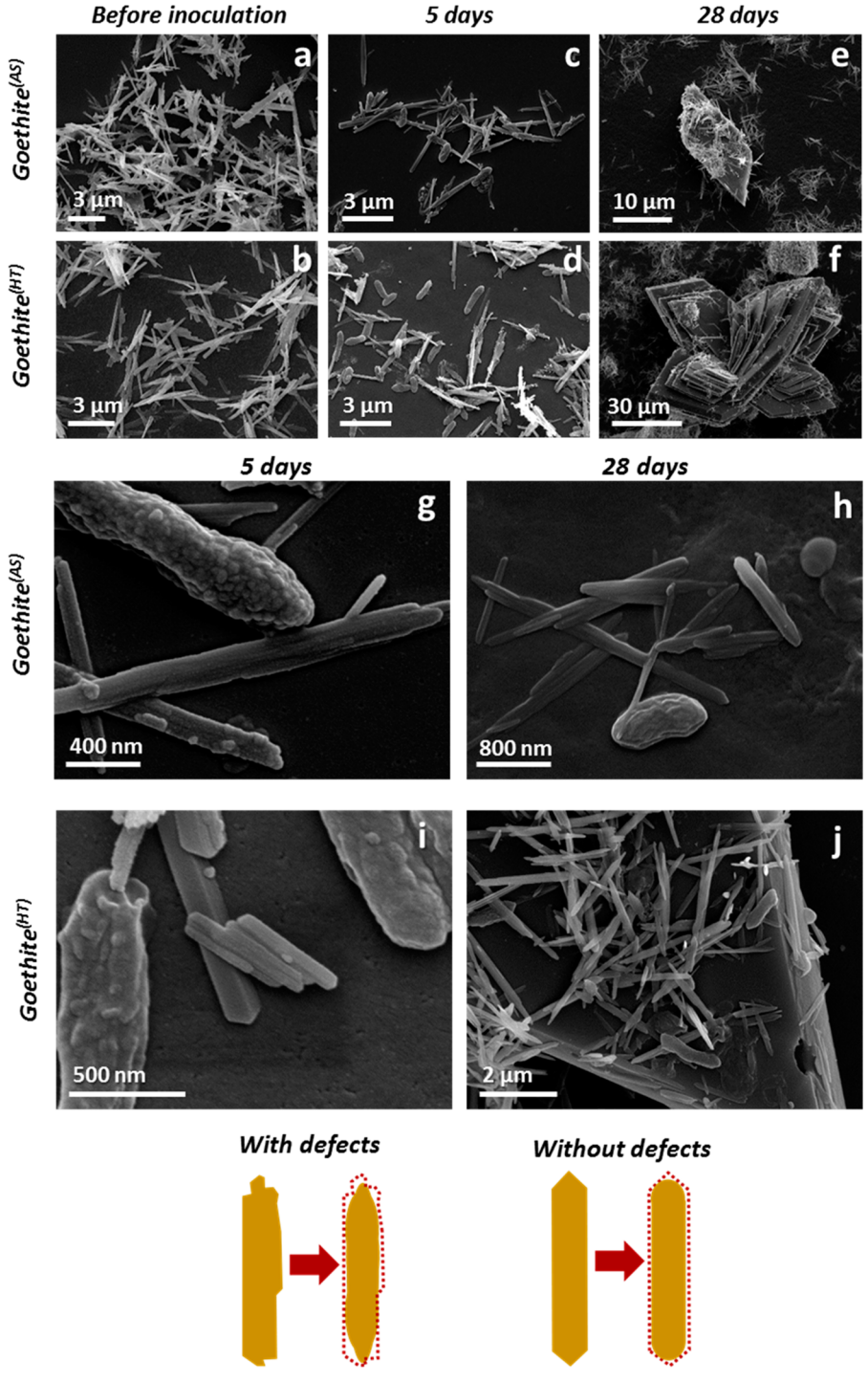

Figure 5. Scanning electron microscopy micrographs of samples of goethite$^{(AS)}$ and goethite$^{(HT)}$ before inoculation (a and b), 5 days after inoculation (c, d, g, and i) and 28 days after inoculation (e, f, h, and j). Experimental conditions: 2 g L^{-1} goethite$^{(AS)}$ or goethite$^{(HT)}$; 10^8 cells mL^{-1} *Geobacter sulfurreducens*; 10 μM AQDS.

together (green shaded area), there seems to be a suppression of the reduction of goethite$^{(HT)}$ and an enhanced reduction of goethite$^{(AS)}$. In fact, for the reduction done separately, 70% of the value is above the line and comes from goethite$^{(AS)}$ (at 16 h). For the reduction done together, 90% of the reduced atoms come from goethite$^{(AS)}$. The different behaviors of reduction when goethite$^{(AS)}$ and goethite$^{(HT)}$ were added together or separately can also be observed in the initial rate of Fe(III) reduction (Figure S6). When reduction happened separately, the rate of reduction of goethite$^{(AS)}$ was 1.67× greater than the rate of goethite$^{(HT)}$. When reduction happened together, the rate of reduction of goethite$^{(AS)}$ was 6.6× greater than the rate of goethite$^{(HT)}$. More reduction of goethite with defects than that predicted by simple linear addition of separate reactors suggests that there is a suppression of the reduction of goethite with fewer defects in favor of the reduction of minerals with more defects.

In the presence of the external electron shuttle AQDS, the enhanced reduction of goethite containing defects seems to be independent of microbial activity. The almost 10-fold increase

DOI: 10.1021/acs.est.9b03208
Environ. Sci. Technol. 2019, 53, 8883−8891

in extent of Fe(III) reduction in the presence of AQDS demonstrates that most electron transfer is happening through the reduced form of AQDS, i.e., AH_2QDS. Interestingly, the chemical constraints for the reduction of goethite with less defects was also observed in our chemically reduced goethite. The comparison of the biological and chemical reduction of goethite revealed a similar isotope signature for both chemically reduced and microbial reduced iron (Figure S1). This result suggests we can use chemical reduction through dithionite to predict the isotope signature of goethite reduced through microbial Fe(III) reduction assisted by an electron shuttle. While the isotope signature is similar for microbial and chemical reduction, the kinetics were different and cannot be used to estimate microbial Fe(III) reduction.

In the absence of AQDS, our reduction experiments (separately) revealed faster initial rates and a greater extent of microbial Fe(III) reduction for goethite$^{(AS)}$ when compared to those of goethite$^{(HT)}$. Therefore, we can speculate that when reduced together in the absence of AQDS, goethite$^{(AS)}$ would also be preferentially reduced. However, additional isotope-labeled microbial Fe(III) reduction experiments without AQDS would be necessary to confirm if the preferential reduction of goethite with defects is also valid when the electron is injected into the Fe(III) mineral directly via enzymatic activity.

Solid Phase Characterization. Approximately 80.0 ± 9% of the Fe(II) formed during goethite reduction was recovered in the 1 M sodium acetate extraction and not in the aqueous phase, suggesting the formation of an Fe(II) precipitate phase (Figure S7). To explore the changes in Fe mineralogy as a result of microbial Fe(III) reduction, we analyzed solid phases of goethite$^{(AS)}$ and goethite$^{(HT)}$ reduced by *Geobacter sulfurreducens* in the presence of AQDS using XRD, Mössbauer spectroscopy, and SEM. XRD diffractograms of samples collected 20 days after incubation revealed vivianite ($Fe_3(PO_4)_2{\cdot}8(H_2O)$) formation (Figure S8). Mössbauer spectroscopy confirmed the formation of vivianite and further revealed that ~19% of the Fe atoms corresponded to vivianite (Figure S9 and Table S1). For both goethites, there was virtually no difference in the amount of vivianite formed when reducing goethite$^{(AS)}$ or goethite$^{(HT)}$ in the presence of the electron shuttle. For the abiotic controls of both minerals, goethite was the only Fe phase identified. Vivianite has been observed in systems in which goethite is reduced through microbial respiration[29,50,51] and can be explained by the high phosphate content in the medium (4.4 mM).[16] The formation of an Fe(II) solid phase possibly limits the inhibitory effect of Fe(II) sorbed onto goethite and may explain the higher extent of goethite reduction in our experiments when compared with previous works.[15,29] XRD analysis of the solids before and after sodium acetate extraction showed a substantial loss in the vivianite peak, demonstrating that most of the vivianite was dissolved after extraction (Figure S10). The ability to recover vivianite with sodium acetate extraction is curious since in natural samples, Fe-bound phosphate is usually extracted with sodium dithionite ($Na_2S_2O_4$),[52] and in similar studies, Fe(II) present in vivianite is usually accounted in the fraction extracted with 0.5 M HCl.[15,29,50] It is possible that not only crystalline vivianite but also some poorly crystalline Fe(II)-phosphate phase was present in the solid phase.

SEM analysis of raw goethite$^{(AS)}$ (Figure 5a) and goethite$^{(HT)}$ (Figure 5b) revealed that goethite$^{(HT)}$ contains more perfectly formed ends. After 5 days of inoculation, there was an abundance of cells in the presence of both goethite$^{(AS)}$ (Figure 5c) and goethite$^{(HT)}$ in the presence of AQDS (Figure 5d). The cells did not seem to be necessarily attached to the minerals suggesting alternative strategies to transfer the electron other than direct contact, which is expected due to the presence of AQDS as an extracellular electron shuttle. After 28 days of incubation, the SEM pictures revealed the presence of large tabular minerals, compatible with vivianite,[50,53] surrounded by needle-like goethite (Figure 5e,f). A closer look at the scanning electron micrographs revealed a substantial change in the morphology of goethite after 28 days of incubation (Figure 5g,h). At the initial incubation stages, goethite$^{(AS)}$ presented "broken" but clear rod ends. When 16.6% of the Fe(III) was reduced, goethite looked scoured and presented rounded ends. Similar changes were observed for goethite$^{(HT)}$ that initially presented perfectly formed ends but later (12.9% of the Fe(III) reduced) presented rounded ends (Figure 5i,j). These results are consistent with previous work that showed that bacterial reduction of structural Fe(III) within goethite possibly occurs preferentially at (021) relative to the (110) and (100) surfaces.[15] The increased reduction of the goethite's ends possibly derives from a preferred reaction of AH_2QDS with the rod's ends. In other studies, the reductant Fe(II) has also been found to have the ends of goethite as preferential reduction sites.[54,55] Similar changes on the shape of goethite ends were observed for goethite$^{(AS)}$ and goethite$^{(HT)}$. Therefore, the preferential reduction at goethite ends sheds light onto the mechanisms of goethite microbial Fe(III) reduction. However, these changes in morphology do not explain the differences that arise upon the presence of defects. The localized reduction, however, may explain why the change in the rate of Fe(III) reduction happened before the entire first layer of Fe atoms could have possibly been removed.

■ ENVIRONMENTAL IMPLICATIONS

Our analysis of the role of defects in the microbial Fe(III) reduction of goethite revealed that the presence of defects results in faster initial reduction rates of microbial Fe(III) reduction but has little/no effect in the extent of Fe(III) reduction after 41 days. In addition, SEM micrographs revealed a preferential reduction on the goethite rods ends. Here, we hypothesize that at the initial stages, the presence of defects plays an important role on the kinetics of goethite reduction, allowing faster reduction of goethite with more defects. However, reduction is localized at the ends of goethite (as shown by SEM), and once the first few layers of atoms at the ends have been removed, reduction is accelerated. Ultimately, the extent of goethite reduction is not influenced by the presence of defects because the kinetic constraints were only relevant in the initial stages while the rods ends were being etched.

In a heterogeneous environment, however, where goethite with defects and with fewer defects are likely to be present together, the initial reduction data suggests the suppression of the reduction of goethite with fewer defects in favor of the reduction of minerals with more defects. These results suggest that while the presence of defects does not affect the rates of microbial reduction in the long term, it will likely determine which minerals will be used as the electron acceptors for Fe(III) reduction. This is true in particular in dynamic systems where Fe(III) minerals, including goethite, are constantly produced and reduced. In such dynamic systems, the short-

DOI: 10.1021/acs.est.9b03208
Environ. Sci. Technol. 2019, 53, 8883−8891

term preferential reduction may ultimately lead to a *frequent* turnover of goethite with more defects, as minerals are constantly being renovated. Perhaps thermodynamic constraints for reduction lead to the preferential reduction of minerals with more defects. The electron transfer from Fe(II) and goethite has been demonstrated to be more favorable in goethite that contains defects,[31] and density functional theory (DFT) calculations showed that surface defects could decrease the activation energy for Fe(II)−goethite electron transfer by reducing the coordination of Fe(III) to lattice oxygen atoms.[56]

Originally, dissimilatory iron reduction of iron minerals was thought to be only possible for short-range ordered minerals, such as ferrihydrite. Later, crystalline Fe(III) minerals, such as goethite, lepidocrocite, hematite, and magnetite, were also found to be suitable for microbial Fe(III) reduction,[3,14−20,57,58] and the rate of reduction was inversely proportional to mineral crystallinity. Our results take this one step further and indicate that even *small* changes at mineral surfaces, such as the presence of surface defects (e.g., Fe vacancies) can enhance bioavailability of goethite toward microbial Fe(III) reduction. Our data further suggests that the reduction of particles with more or less defects is not simply a linear combination of the reduction of the particles separately but is instead a preferential use of Fe(III) minerals with defects as the electron acceptors for microbial respiration.

■ ASSOCIATED CONTENT

Supporting Information

The Supporting Information is available free of charge on the ACS Publications website at DOI: 10.1021/acs.est.9b03208.

Details on Mössbauer fitting, XRD, additional methods details, discussion on composition of the sodium acetate extraction, calculations of the isotopes, calculation of the surface area, calculation of the rates of Fe(III) reduction (PDF)

■ AUTHOR INFORMATION

Corresponding Author

*Phone: +49-(0)7071-29-74992. Fax: +49-(0)7071-29-5059. E-mail: andreas.kappler@uni-tuebingen.de.

ORCID

Luiza Notini: 0000-0003-2972-6588
James M. Byrne: 0000-0002-4399-7336
Drew E. Latta: 0000-0001-9414-5590
Zhe Zhou: 0000-0001-7732-9582
Andreas Kappler: 0000-0002-3558-9500

Notes

The authors declare no competing financial interest.

■ ACKNOWLEDGMENTS

This material is based upon work supported by the German Academic Exchange Service (DAAD) Short-Term Research Grant 2018 and by the University of Iowa Graduate College T. Anne Cleary International Dissertation Research Fellowship. Additional support for this work was provided by the NSF Division of Graduate Education under Grant No. 1633098.

■ REFERENCES

(1) Roden, E. E. Geochemical and microbiological controls on dissimilatory iron reduction. *C. R. Geosci.* **2006**, *338* (6), 456−467.

(2) Roden, E. E.; Urrutia, M. M. Influence of biogenic Fe (II) on bacterial crystalline Fe (III) oxide reduction. *Geomicrobiol. J.* **2002**, *19* (2), 209−251.

(3) Roden, E. E.; Zachara, J. M. Microbial Reduction of Crystalline Iron(III) Oxides: Influence of Oxide Surface Area and Potential for Cell Growth. *Environ. Sci. Technol.* **1996**, *30* (5), 1618−1628.

(4) Lloyd, J. R. Microbial reduction of metals and radionuclides. *FEMS Microbiol. Rev.* **2003**, *27* (2−3), 411−425.

(5) Weber, K. A.; Achenbach, L. A.; Coates, J. D. Microorganisms pumping iron: anaerobic microbial iron oxidation and reduction. *Nat. Rev. Microbiol.* **2006**, *4* (10), 752−764.

(6) Murray, G. C.; Hesterberg, D. Iron and phosphate dissolution during abiotic reduction of ferrihydrite-boehmite mixtures. *Soil Sci. Soc. Am. J.* **2006**, *70* (4), 1318−1327.

(7) Matocha, C. J.; Dhakal, P.; Pyzola, S. M., Chapter Four - The Role of Abiotic and Coupled Biotic/Abiotic Mineral Controlled Redox Processes in Nitrate Reduction. In *Adv. Agron.*, Donald, L. S., Ed. Academic Press: 2012; Vol. *115*, pp 181−214.

(8) Van Cleemput, O. Subsoils: chemo-and biological denitrification, N2O and N2 emissions. *Nutr. Cycling Agroecosyst.* **1998**, *52* (2−3), 187−194.

(9) Ernstsen, V. Reduction of Nitrate by Fe^{2+} in Clay Minerals. *Clays Clay Miner.* **1996**, *44* (5), 599−608.

(10) Colombo, C.; Palumbo, G.; He, J.-Z.; Pinton, R.; Cesco, S. Review on iron availability in soil: interaction of Fe minerals, plants, and microbes. *J. Soils Sediments* **2014**, *14* (3), 538−548.

(11) Stumm, W.; Sulzberger, B. The cycling of iron in natural environments: Considerations based on laboratory studies of heterogeneous redox processes. *Geochim. Cosmochim. Acta* **1992**, *56* (8), 3233−3257.

(12) Jickells, T. Atmospheric inputs of metals and nutrients to the oceans: their magnitude and effects. *Mar. Chem.* **1995**, *48*, 199−214.

(13) Lovley, D. R.; Phillips, E. J. P. Novel Mode of Microbial Energy Metabolism: Organic Carbon Oxidation Coupled to Dissimilatory Reduction of Iron or Manganese. *Appl. Environ. Microbiol.* **1988**, *54* (6), 1472−1480.

(14) Kashyap, S.; Sklute, E. C.; Dyar, M. D.; Holden, J. F. Reduction and Morphological Transformation of Synthetic Nanophase Iron Oxide Minerals by Hyperthermophilic Archaea. *Front. Microbiol.* **2018**, *9*, 1550−1550.

(15) Cutting, R. S.; Coker, V. S.; Fellowes, J. W.; Lloyd, J. R.; Vaughan, D. J. Mineralogical and morphological constraints on the reduction of Fe(III) minerals by Geobacter sulfurreducens. *Geochim. Cosmochim. Acta* **2009**, *73* (14), 4004−4022.

(16) Miot, J.; Etique, M., Formation and transformation of iron-bearing minerals by iron (II)-oxidizing and iron (III)-reducing bacteria. In *Iron Oxides: From Nature to Applications*; 2016; pp 53−98.

(17) Hansel, C. M.; Benner, S. G.; Nico, P.; Fendorf, S. Structural constraints of ferric (hydr)oxides on dissimilatory iron reduction and the fate of Fe(II)33Associate editor: J. B. Fein. *Geochim. Cosmochim. Acta* **2004**, *68* (15), 3217−3229.

(18) Hori, T.; Aoyagi, T.; Itoh, H.; Narihiro, T.; Oikawa, A.; Suzuki, K.; Ogata, A.; Friedrich, M. W.; Conrad, R.; Kamagata, Y. Isolation of microorganisms involved in reduction of crystalline iron (III) oxides in natural environments. *Front. Microbiol.* **2015**, *6*, 386.

(19) O'Loughlin, E.; Gorski, C.; Scherer, M. Effects of phosphate on secondary mineral formation during the bioreduction of akaganeite (β-FeOOH): Green rust versus framboidal magnetite. *Curr. Inorg. Chem.* **2015**, *5* (3), 214−224.

(20) Loyaux-Lawniczak, S.; Vuilleumier, S.; Geoffroy, V. A. Efficient Reduction of Iron Oxides by Paenibacillus spp. Strains Isolated from Tropical Soils. *Geomicrobiol. J.* **2019**, *36* (5), 423−432.

(21) Melton, E. D.; Swanner, E. D.; Behrens, S.; Schmidt, C.; Kappler, A. The interplay of microbially mediated and abiotic reactions in the biogeochemical Fe cycle. *Nat. Rev. Microbiol.* **2014**, *12* (12), 797−808.

(22) Downie, H. F.; Standerwick, J. P.; Burgess, L.; Natrajan, L. S.; Lloyd, J. R. Imaging redox activity and Fe(II) at the microbe-mineral

DOI: 10.1021/acs.est.9b03208
Environ. Sci. Technol. 2019, 53, 8883−8891

interface during Fe(III) reduction. *Res. Microbiol.* **2018**, *169* (10), 582−589.
(23) Nevin, K. P.; Lovley, D. R. Potential for Nonenzymatic Reduction of Fe(III) via Electron Shuttling in Subsurface Sediments. *Environ. Sci. Technol.* **2000**, *34* (12), 2472−2478.
(24) Reguera, G.; McCarthy, K. D.; Mehta, T.; Nicoll, J. S.; Tuominen, M. T.; Lovley, D. R. Extracellular electron transfer via microbial nanowires. *Nature* **2005**, *435*, 1098−1101.
(25) Roden, E. E.; Kappler, A.; Bauer, I.; Jiang, J.; Paul, A.; Stoesser, R.; Konishi, H.; Xu, H. Extracellular electron transfer through microbial reduction of solid-phase humic substances. *Nat. Geosci.* **2010**, *3*, 417−421.
(26) Jiang, J.; Kappler, A. Kinetics of microbial and chemical reduction of humic substances: implications for electron shuttling. *Environ. Sci. Technol.* **2008**, *42* (10), 3563−3569.
(27) Lentini, C.; Wankel, S.; Hansel, C. Enriched Iron(III)-Reducing Bacterial Communities are Shaped by Carbon Substrate and Iron Oxide Mineralogy. *Front. Microbiol.* **2012**, *3* (404), 1−19.
(28) Urrutia, M. M.; Roden, E. E.; Fredrickson, J. K.; Zachara, J. M. Microbial and surface chemistry controls on reduction of synthetic Fe(III) oxide minerals by the dissimilatory iron-reducing bacterium Shewanella alga. *Geomicrobiol. J.* **1998**, *15* (4), 269−291.
(29) Muehe, E. M.; Scheer, L.; Daus, B.; Kappler, A. Fate of Arsenic during Microbial Reduction of Biogenic versus Abiogenic As−Fe(III)−Mineral Coprecipitates. *Environ. Sci. Technol.* **2013**, *47* (15), 8297−8307.
(30) Callister, W. D.; Rethwisch, D. G. *Materials science and engineering: an introduction*. 9 ed.; Wiley: 2014.
(31) Notini, L.; Latta, D. E.; Neumann, A.; Pearce, C. I.; Sassi, M.; N'Diaye, A. T.; Rosso, K. M.; Scherer, M. M. The Role of Defects in Fe(II)−Goethite Electron Transfer. *Environ. Sci. Technol.* **2018**, *52* (5), 2751−2759.
(32) Yuan, K.; Lee, S. S.; Cha, W.; Ulvestad, A.; Kim, H.; Abdilla, B.; Sturchio, N. C.; Fenter, P. Oxidation induced strain and defects in magnetite crystals. *Nat. Commun.* **2019**, *10* (1), 703.
(33) Taylor, S. D.; Liu, J.; Zhang, X.; Arey, B. W.; Kovarik, L.; Schreiber, D. K.; Perea, D. E.; Rosso, K. M. Visualizing the iron atom exchange front in the Fe (II)-catalyzed recrystallization of goethite by atom probe tomography. *Proc. Natl. Acad. Sci. U. S. A.* **2019**, *116* (8), 2866−2874.
(34) Zarzycki, P.; Rosso, K. M. Energetics and the Role of Defects in Fe(II)-Catalyzed Goethite Recrystallization from Molecular Simulations. *ACS Earth Space Chem.* **2019**, *3* (2), 262−272.
(35) Schwertmann, U.; Cornell, R. M., Goethite. In *Iron Oxides in the Laboratory*; Wiley-VCH Verlag GmbH: 2007; pp 67−92.
(36) Cwiertny, D. M.; Handler, R. M.; Schaefer, M. V.; Grassian, V. H.; Scherer, M. M. Interpreting nanoscale size-effects in aggregated Fe-oxide suspensions: Reaction of Fe(II) with Goethite. *Geochim. Cosmochim. Acta* **2008**, *72* (5), 1365−1380.
(37) Latta, D. E.; Bachman, J. E.; Scherer, M. M. Fe Electron Transfer and Atom Exchange in Goethite: Influence of Al-Substitution and Anion Sorption. *Environ. Sci. Technol.* **2012**, *46* (19), 10614−10623.
(38) Pasakarnis, T.; McCormick, M. L.; Parkin, G. F.; Thompson, A.; Scherer, M. M. Fe^{II}aq−Fe^{III}oxide electron transfer and Fe exchange: effect of organic carbon. *Environ. Chem.* **2015**, *12* (1), 52−63.
(39) Williams, A. G. B.; Scherer, M. M. Spectroscopic Evidence for Fe(II)−Fe(III) Electron Transfer at the Iron Oxide−Water Interface. *Environ. Sci. Technol.* **2004**, *38* (18), 4782−4790.
(40) Handler, R. M.; Beard, B. L.; Johnson, C. M.; Scherer, M. M. Atom Exchange between Aqueous Fe(II) and Goethite: An Fe Isotope Tracer Study. *Environ. Sci. Technol.* **2009**, *43* (4), 1102−1107.
(41) Handler, R. M.; Frierdich, A. J.; Johnson, C. M.; Rosso, K. M.; Beard, B. L.; Wang, C.; Latta, D. E.; Neumann, A.; Pasakarnis, T.; Premaratne, W. A. P. J.; Scherer, M. M. Fe(II)-Catalyzed Recrystallization of Goethite Revisited. *Environ. Sci. Technol.* **2014**, *48* (19), 11302−11311.
(42) Tamura, H.; Goto, K.; Yotsuyanagi, T.; Nagayama, M. Spectrophotometric determination of iron(II) with 1,10-phenanthroline in the presence of large amounts of iron(III). *Talanta* **1974**, *21* (4), 314−318.
(43) Zeitvogel, F.; Burkhardt, C. J.; Schroeppel, B.; Schmid, G.; Ingino, P.; Obst, M. Comparison of Preparation Methods of Bacterial Cell-Mineral Aggregates for SEM Imaging and Analysis Using the Model System of Acidovorax sp. BoFeN1. *Geomicrobiol. J.* **2017**, *34* (4), 317−327.
(44) Ehrlich, H. L.; Newman, D. K.; Kappler, A. *Ehrlich's geomicrobiology*. CRC press: 2015.
(45) Middelburg, J. J.; Boschker, H. T. S. Stable isotopes and biomarkers in microbial ecology. *FEMS Microbiol. Ecol.* **2002**, *40* (2), 85−95.
(46) Johnson, C. M.; Roden, E. E.; Welch, S. A.; Beard, B. L. Experimental constraints on Fe isotope fractionation during magnetite and Fe carbonate formation coupled to dissimilatory hydrous ferric oxide reduction. *Geochim. Cosmochim. Acta* **2005**, *69* (4), 963−993.
(47) Crosby, H. A.; Johnson, C. M.; Roden, E. E.; Beard, B. L. Coupled Fe(II)−Fe(III) Electron and Atom Exchange as a Mechanism for Fe Isotope Fractionation during Dissimilatory Iron Oxide Reduction. *Environ. Sci. Technol.* **2005**, *39* (17), 6698−6704.
(48) Roden, E. E. Fe(III) Oxide Reactivity ward Biological versus Chemical Reduction. *Environ. Sci. Technol.* **2003**, *37* (7), 1319−1324.
(49) Prélot, B.; Villiéras, F.; Pelletier, M.; Gérard, G.; Gaboriaud, F.; Ehrhardt, J.-J.; Perrone, J.; Fedoroff, M.; Jeanjean, J.; Lefèvre, G.; Mazerolles, L.; Pastol, J.-L.; Rouchaud, J.-C.; Lindecker, C. Morphology and surface heterogeneities in synthetic goethites. *J. Colloid Interface Sci.* **2003**, *261* (2), 244−254.
(50) Muehe, E. M.; Morin, G.; Scheer, L.; Pape, P. L.; Esteve, I. n.; Daus, B.; Kappler, A. Arsenic (V) incorporation in vivianite during microbial reduction of arsenic (V)-bearing biogenic Fe (III)(oxyhydr) oxides. *Environ. Sci. Technol.* **2016**, *50* (5), 2281−2291.
(51) Najem, T.; Langley, S.; Fortin, D. A comparison of Fe(III) reduction rates between fresh and aged biogenic iron oxides (BIOS) by Shewanella putrefaciens CN32. *Chem. Geol.* **2016**, *439*, 1−12.
(52) Lukkari, K.; Hartikainen, H.; Leivuori, M. Fractionation of sediment phosphorus revisited. I: Fractionation steps and their biogeochemical basis. *Limnol. Oceanogr.: Methods* **2007**, *5* (12), 433−444.
(53) Sánchez-Román, M.; Puente-Sánchez, F.; Parro, V.; amils, R. Nucleation of Fe-rich phosphates and carbonates on microbial cells and exopolymeric substances. *Front. Microbiol.* **2015**, *6* (1024), 1−9.
(54) Joshi, P.; Gorski, C. A. Anisotropic Morphological Changes in Goethite during Fe^{2+}-Catalyzed Recrystallization. *Environ. Sci. Technol.* **2016**, *50* (14), 7315−7324.
(55) Southall, S. C.; Micklethwaite, S.; Wilson, S. A.; Frierdich, A. J. Changes in Crystallinity and Tracer-Isotope Distribution of Goethite during Fe(II)-Accelerated Recrystallization. *ACS Earth Space Chem.* **2018**, *2* (12), 1271−1282.
(56) Alexandrov, V.; Rosso, K. M. Ab initio modeling of Fe(II) adsorption and interfacial electron transfer at goethite (α-FeOOH) surfaces. *Phys. Chem. Chem. Phys.* **2015**, *17* (22), 14518−14531.
(57) Kostka, J. E.; Nealson, K. H. Dissolution and Reduction of Magnetite by Bacteria. *Environ. Sci. Technol.* **1995**, *29* (10), 2535−2540.
(58) Byrne, J. M.; Klueglein, N.; Pearce, C.; Rosso, K. M.; Appel, E.; Kappler, A. Redox cycling of Fe(II) and Fe(III) in magnetite by Fe-metabolizing bacteria. *Science* **2015**, *347* (6229), 1473−1476.

DOI: 10.1021/acs.est.9b03208
Environ. Sci. Technol. 2019, 53, 8883−8891